Journal of Zhejiang University-SCIENCE C (Computers & Electronics)
ISSN 1869-1951 (Print); ISSN 1869-196X (Online)
www.zju.edu.cn/jzus; www.springerlink.com
E-mail: jzus@zju.edu.cn

A vehicle re-identification algorithm based on multi-sensor correlation*

Yin TIAN[†1], Hong-hui DONG[1], Li-min JIA[†‡1], Si-yu LI[2]

([1]*State Key Laboratory of Rail Traffic Control and Safety, Beijing Jiaotong University, Beijing 100044, China*)

([2]*Shenzhen Graduate School, Peking University, Shenzhen 518055, China*)

[†]E-mail: 10114241@bjtu.edu.cn; lmjia@bjtu.edu.cn

Received Oct. 16, 2013; Revision accepted Feb. 10, 2014; Crosschecked Apr. 11, 2014

Abstract: Magnetic sensors can be applied in vehicle recognition. Most of the existing vehicle recognition algorithms use one sensor node to measure a vehicle's signature. However, vehicle speed variation and environmental disturbances usually cause errors during such a process. In this paper we propose a method using multiple sensor nodes to accomplish vehicle recognition. Based on the matching result of one vehicle's signature obtained by different nodes, this method determines vehicle status and corrects signature segmentation. The co-relationship between signatures is also obtained, and the time offset is corrected by such a co-relationship. The corrected signatures are fused via maximum likelihood estimation, so as to obtain more accurate vehicle signatures. Examples show that the proposed algorithm can provide input parameters with higher accuracy. It improves the average accuracy of vehicle recognition from 94.0% to 96.1%, and especially the bus recognition accuracy from 77.6% to 92.8%.

Key words: Vehicle re-identification, Magnetic sensor network, Correlation, Cross matching
doi:10.1631/jzus.C1300291 **Document code:** A **CLC number:** TP212.9

1 Introduction

Automatic vehicle identification (AVI) is one of the key parts of an intelligent transportation system (ITS). It supports automatic operation of ITS by providing various data, such as real-time travel time information (Tam and Lam, 2011), drivers' headway preference (Gunay, 2012), real-time crash prediction (Ahmed and Abdel-Aty, 2012), signalized intersection delays (Sharma *et al.*, 2007). The earliest AVI system appeared in the 1980s. It applied optical character recognition (OCR) techniques to photograph the license plates (Lotufo *et al*., 1990). Mature applications of AVI systems are generalized as follows: vehicle signatures are obtained through different types of sensors, and vehicles are identified via pattern recognition.

Currently, three major types of equipment are used to obtain vehicle signatures: induction loop detector (ILD), magnetic sensor, and video camera. ILD has a simple principle and low cost, so it is the most widely used sensor and has been frequently applied to large-scale engineering. However, ILD is improper for vehicle identification, because its low sensitivity and poor noise immunity cannot satisfy the accuracy requirement. The rationale of vehicle identification by video camera is, distinguishing vehicles through analyzing license plate numbers and car shape. It is more accurate than ILD, but the cost of video recognition is high and a large volume of data will be generated, which requires high performance of transmission and computation. In addition, a video camera approach may infringe on privacy. If data is leaked, security issues will occur. The method of using magnetic sensors is a novel approach proposed by a research team at UC Berkeley (Cheung *et al*., 2005). It uses sensors buried underground to conduct

‡ Corresponding author

* Project supported by the National Natural Science Foundation of China (No. 61104164) and the National High-Tech R&D Program (863) of China (No. 2012AA112401)

identification. Those sensors identify the magnetic signals of different vehicles, and obtain information such as speed, vehicle type, and occupancy. Magnetic sensors are small, power saving, and highly sensitive, so they are easy to install and maintain. Moreover, there will be no privacy disclosure problem.

Today, vehicle identification based on magnetic sensors has progressed enormously. For example, the wireless magnetic sensor network at UC Berkeley matches vehicle features by analyzing the length of the vehicle. Its identification accuracy is about 75% (Cheung *et al*., 2005). In the VSN240 system, the adaptive threshold detection algorithm (ATDA) proposed by UC Berkeley has been adopted to identify vehicles and achieves an accuracy of 71% (Cheung and Varaiya, 2007). The binary proximity sensor networks (BPSNs) suggested by Dalian University of Technology apply the binary proximity algorithm and obtain an accuracy of 93.61% (Zhang *et al*., 2008). The wireless magnetic sensor from Chulalongkorn University identified buses with an accuracy of 80%, and passenger cars with an accuracy of 68% (Keawkamnerd *et al*., 2008; Kaewkamnerd *et al*., 2009).

According to the existing systems, vehicle identification errors are generally ascribed to two types of situation: (1) when the traffic flow is unblocked, systems may misidentify a bus as several passenger cars; (2) when the traffic flow is congested, in addition to the former error, two passenger cars very close to each other may most likely be identified as a bus.

Until now, there have been few solutions to deal with these two types of vehicle identification errors. The magnetic sensors applied in existing research are based mainly on 'point' measures, so only one point can be reflected at one time. In fact, magnetic sensors are ideal for constituting wireless sensor networks. They can obtain vehicle identification data with higher accuracy by finding the spatio-temporal correlations of multiple sensor nodes. There were studies using such correlations to re-identify vehicles so as to obtain the average travel time on certain roads (Kwong *et al*., 2009), but they seldom emphasized specific vehicle classification. Some other studies tried to analyze the spatio-temporal correlations of vehicle signatures from different nodes in a network (Abdulhai and Tabib, 2003). Although the stimulation result was not ideal, this kind of idea makes sense.

Ndoye *et al*. (2011a) proposed an algorithm that takes advantage of multiple sensors to deal with the loop signature re-identification problem in intelligent imaging systems, in which the loops were installed in a 'loop-trap' configuration. This algorithm has high accuracy for vehicle re-identification. However, as it focuses on how to obtain the travel time, modification to the algorithm is necessary for specific use in vehicle recognition.

In this paper we propose a multi-sensor spatio-temporal correlation algorithm for vehicle re-identification. This algorithm can provide input parameters that are more effective for vehicle recognition, which improves the recognition accuracy. This algorithm relies on a magnetic wireless sensor network that contains several independent magnetic sensor nodes connected by wireless communication. Data is transmitted to an access point (AP) which has certain computability. Identification errors can be reduced by fusing information from multiple nodes. The more accurate data can provide support for various kinds of applications, such as road access restriction management, vehicle guidance in a parking lot, road safety monitoring, and the highway toll charge model. Moreover, since only vehicle signature is obtained, there will be no offense to privacy. As there has been a large amount of research discussing vehicle identification algorithms, the identification process is not the focus of this paper. Instead, the issue addressed is how to provide vehicle signatures with higher accuracy for vehicle identification algorithms. The advantages of our proposed algorithm are: (1) it requires fewer sensors to extract the signatures of a vehicle, i.e., only two sensors for each lane; (2) it improves the accuracy of the vehicle re-identification algorithm by considering actual traffic flow; (3) it further improves the identification accuracy using the fusion algorithm based on maximum likelihood estimation to filter vehicle feature signals.

2 Magnetic wireless sensor network and experimental environment

By measuring the change of the magnetic field, signatures of different vehicles can be obtained. This is because different configurations and wear degrees will lead to different spatial distributions of the ferromagnetic material. When vehicles pass a same

fixed point, the magnetic field will be influenced differently. The magnetic sensor nodes used in this study consisted of a magneto-resistive sensor, a microprocessor board with 512 MB memory, a radio transceiver, an antenna, and a battery. All of these components were packaged in a polycarbonate case cylinder of 100 mm diameter and 64 mm height, and filled with epoxy. The sampling rate of the three axes of the Earth's magnetic field was 300 Hz. Since only the *z*-axis data was needed, nodes were set to send only raw data on the *z*-axis to the APs. Each node had an independent IP address. APs were connected with a ZigBee at 2.4 GHz. Each AP had a dual-core processing core at 2.9 GHz, 4 GB memory, 512 GB SSD, AC power supply, coverage of 500 m, supporting access to 255 nodes simultaneously, and could satisfy the computing needs of various data analysis algorithms.

The experiment system was located at Jiao Da Dong Lu, Haidian District, Beijing, a two-way road with a single lane on each side. The experiment was conducted on a section of 226 m long road heading from south to north. A node was set separately at the downstream and the upstream. The layout and location are exhibited in Fig. 1.

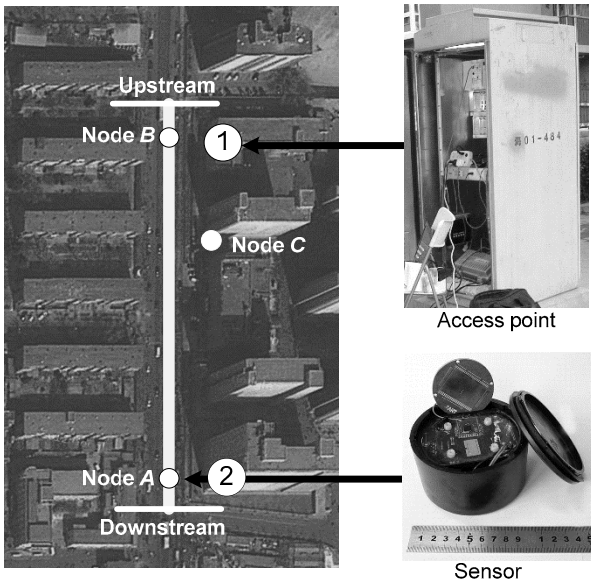

Fig. 1 Schematic of sensor nodes, the access point, and the installation location

According to Kwong *et al*. (2009), the nodes were placed 12 m from the intersection. *A* and *B* are sensor nodes, *C* is the access point, and two video cameras were placed at '1' and '2'. The test time was from Jan. 20, 2013 to Jan. 23, 2013. The test process was calibrated with video data

The basis of vehicle re-identification is the segmentation of the vehicle signatures. Each type of vehicle has its particular signature. Fig. 2 shows the two typical waveforms of the vehicle signature obtained by node *A*. Fig. 2a exhibits the waveform when a passenger car passes, while Fig. 2b is the waveform when a bus with 45 seats passes. The datum line α stands for the average value of output data from that node in a period of 5 min, when there is not a vehicle within an area of 50 m radius around that sensor. Notice that, when the outputs of the magnetoresistive sensors inside the nodes are directly read, there will be some high-frequency noise influencing the recognition accuracy. To improve the efficiency of identification by the nodes, a first-order low-pass filter was added. Experimental results show that the best cutoff frequency of that filter is 3000 Hz.

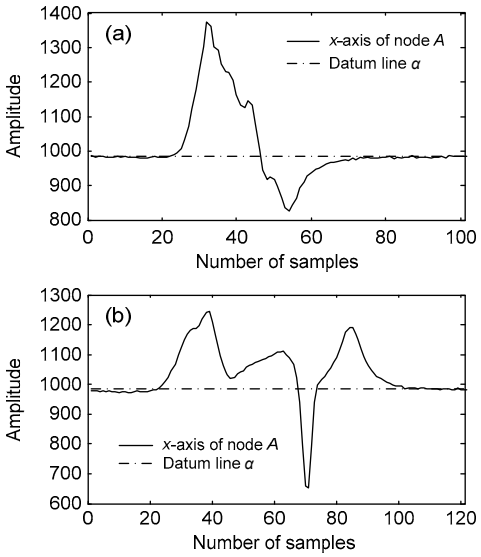

Fig. 2 The raw *z*-axis magnetic signal generated by vehicle signature: (a) vehicle signature of a passenger car; (b) vehicle signature of a bus with 45 seats

To verify the accuracy of the proposed multi-sensor system, a reference system is needed. Currently, there are various methods using the magnetic sensors data to identify vehicles (Cheung *et al*., 2005; Keawkamnerd *et al*., 2008; Zhang *et al*., 2008). Almost all of the existing algorithms for vehicle identification are based on a single node. The effectiveness of the proposed algorithm is verified by data obtained from node *A*. The data of the 4-day experiment is the inputs of the identification

algorithm (Zhang *et al*., 2008). The automatic identification results are compared with the video calibration data (Table 1). The standard of vehicle identification is referred to the FHWA (Federal Highway Administration, USA) scheme (DOT/ NHTSA, April 5, 2012).

Table 1 The accuracy of vehicle identification by a single-point sensor node system

Vehicle type	Number of vehicles		Accuracy
	Single node identification	Actual	
Bus	996	1284	77.6%
Car	15088	15668	96.3%
Truck	384	516	74.4%
Van	1736	1888	91.9%
Total	18204	19356	94.0%

Table 1 shows that the proposed algorithm performs better in identifying passenger cars than identifying buses. This result is consistent with the outcome in Zhang *et al*. (2008). It is necessary to analyze errors generated by automatic identification so as to improve the identification accuracy. Comparison with video calibration data shows that 78.2% of the errors are caused by misidentification of a bus as several passenger cars, and 21.8% by misidentification of several passenger cars as a bus. The former type of error mostly occurs when vehicle speed is low, while the latter type of error is common in traffic congestion. For a single node system, there are two ways to reduce these errors: one is using sensors with high precision, and the other is resorting to a better algorithm. However, such improvements greatly increase the burden of the system, and are hard to achieve. To reduce the identification error, in this study we create a method using multiple sensor nodes in one system to re-identify vehicles.

Currently, there are multiple methods for vehicle re-identification. One is using a camera to obtain the shape of a vehicle and then extracting vehicle signatures based on its shape (Gandhi and Trivedi, 2006). The shortcoming of this method is that, it demands high computing capability and is not suitable for roadside equipment for long-term use. The other method to re-identify vehicles is by comparing vehicle lengths (Coifman, 1998). This method effectively mitigates the computational complexity. It has poor accuracy, however, as it classifies vehicles based only on length. Some researchers proposed a method of installing a pair of sensors at each intersection, and then identifying vehicles based on the interrelation between these sensors (Kwong *et al*., 2009). The drawback of this method is the high cost, since every intersection needs four sensors. To address the shortcomings above, we propose a method and give the related algorithm for vehicle re-identification, which are prospective in practical applications.

3 Description of the multi-sensor spatio-temporal correlation algorithm

In the AVI system which consists of multiple sensor nodes, there is a strong correlation between the signatures obtained by these nodes. Such correlations are used by the algorithm proposed in this paper to enhance and fuse vehicle signatures. Based on the fusion result, accurate vehicle signature waveforms are obtained to correct recognition errors. The multi-sensor spatio-temporal correlation algorithm is proposed which contains four parts: data collection and interpolation, data error estimation, waveform matching, and waveform fusion. Each part will be detailed in the following.

3.1 Data collection and interpolation

The experimental section is a single lane, and each vehicle has to pass both node *A* and node *B*. Therefore, data from nodes *A* and *B* has a certain spatio-temporal correlation, which can be used to enhance and fuse the vehicle signature. Node *A* (located at the downstream of the intersection) was 202 m (d=202 m) away from node *B* (located at the upstream of the intersection). Suppose that the maximum speed of the vehicles on this section is 80 km/h. So, the minimum time for a vehicle to pass the whole section is 9 s, and the time synchronization accuracy of the two nodes is at a millisecond level, which is easy to acquire for a sensor network. The sampling time and system time of points recorded by nodes are described as $\{t^n_{\mathrm{p},l}(k): l=1,2,\cdots,100,\ k\geq 0\}$ and $\{t^n_{\mathrm{s},k}: k\geq 0\}$, respectively, with n representing the number of nodes and l the time offset of the sampling points. The relationship between system time and sampling point time can be described as

$$t^n_{\mathrm{s},k} \le t^n_{\mathrm{p},1}(k)<t^n_{\mathrm{p},2}(k)<\cdots<t^n_{\mathrm{p},100}(k) \le t^n_{\mathrm{s},k+1}. \quad (1)$$

The magnetic field amplitude E^n obtained by node n is

$$E^n = \{\tilde{\delta}(t^n_{\mathrm{p},l}(k)): l=1, 2, \cdots, 100, k \ge 0\}. \quad (2)$$

After obtaining the data of the magnetic field, the next step is vehicle detection, i.e., using proper algorithms to segment vehicle signature waveforms collected by the sensors. It can be concluded from Fig. 2 that, with the forward portion of a vehicle, there will be a significant offset between the waveform and the datum line α, while with the vehicle leaving, the waveform will overlap with α again. Therefore, the dual-window vehicle detection algorithm is proper for obtaining waveform data (Haoui *et al*., 2008). For an arbitrary vehicle v, its signature waveform E^N_v is

$$E^n_v = \{\tilde{\delta}(t^n_{\mathrm{p},l}(k)) : t^n_{\mathrm{v,in}} \le t^n_{\mathrm{p},l}(k) \le t^n_{\mathrm{v,out}}\} \quad (3)$$

$$\text{s.t.} \quad t^n_{v,\mathrm{in}} = t^n_{\mathrm{p},l}(k), \quad (4)$$

$$t^n_{v,\mathrm{out}} = t^n_{\mathrm{p},l}(k+\Delta), \quad (5)$$

$$E^n_v \in E^n, \quad (6)$$

$$k \ge 0, \quad (7)$$

$$\Delta \ge 0, \quad (8)$$

where $t^n_{v,\mathrm{in}}$ is the starting time of vehicle v's waveform, and $t^n_{v,\mathrm{out}}$ means the ending time.

Even for the same vehicle, waveforms will be different since its passing speed varies from sensor to sensor. Normalization of the waveform is necessary to facilitate further data analysis. During interval T_d, among all of the passing vehicles, there is one that spends the longest time. Setting its time $t_{\mathrm{d,max}}=\max(t^n_{v,\mathrm{out}}-t^n_{v,\mathrm{in}})$ as the datum, and interpolating the waveforms of the remaining vehicles, the piecewise cubic Hermite interpolant polynomial (PCHIP) method (Fritsch and Carlson, 1980) is applied to obtain accurate waveforms. After this process, waveforms of all vehicles have the same projection on the x-axis of the Cartesian coordinate system, which is described as

$$\|\boldsymbol{E}_v\| = t_{\mathrm{d,max}}. \quad (9)$$

3.2 Data error estimation

Set τ_n as the registration error of n, and ω_n the environmental noise of node N. Concluding from the environmental noise analysis, ω_n is white Gaussian noise superimposed on the vehicle signature waveform. Errors τ_n generated by each registration process are independent and identically distributed discrete random variables. The mean is zero and the variance is finite (Ndoye *et al*., 2011b). Therefore, when T_d is large enough, i.e., there are enough sampling nodes, there is

$$\frac{1}{N}\sum_{n=1}^{N}\tau_n \approx 0. \quad (10)$$

According to the law of large numbers, the data error will be corrected via synchronization, filtering, and fusion after multiple sampling.

3.3 Vehicle signature cross matching

After signal processing, vehicle signatures from different nodes are to be matched to obtain the spatio-temporal correlations of the signals. Data matching consists of a matching strategy and a matching algorithm, which will be explained in the following.

Considering the experiment scene of this study: vehicles enter from node A and leave from node B. According to the video calibration data, the statuses of entering vehicles can be classified into three types:

1. Follow the front vehicle until leaving the section.

2. Overtake one or more vehicles before leaving the section.

3. Park on the temporary parking curb.

Meanwhile, there are two kinds of errors in vehicle identification:

(a) All nodes misidentify a bus as several passenger cars;

(b) Only one node misidentifies the vehicle type while others correctly identify the vehicle type.

All situations above are summarized in Fig. 3.

Each situation and the related discriminant are described in the following.

$E^A_1 \to E^B_1$ is status 1. The discriminant is: calculating the Pearson correlation coefficient ρ_{ij} between the vehicle j detected by node B and the vehicle i detected by node A.

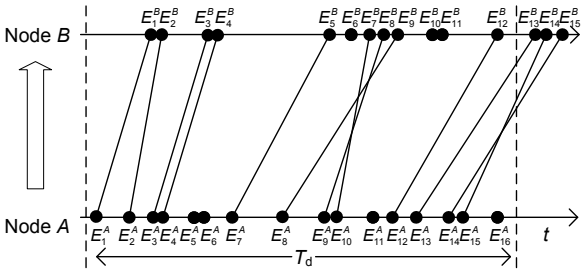

Fig. 3 The errors in vehicle signature matching

$$\rho_{ij}=\frac{\sum E_i^A E_j^B-\dfrac{\sum E_i^A \sum E_j^B}{\|\boldsymbol{E}_v\|}}{\sqrt{\sum (E_i^A)^2-\dfrac{\left(\sum E_i^A\right)^2}{\|\boldsymbol{E}_v\|}}\sqrt{\sum (E_j^B)^2-\dfrac{\left(\sum E_j^B\right)^2}{\|\boldsymbol{E}_v\|}}}. \tag{11}$$

Crossly compare all vehicle entering and leaving, and obtain the correlation matrix $\boldsymbol{\Theta}$:

$$\boldsymbol{\Theta}=\begin{bmatrix}\rho_{11} & \rho_{12} & \cdots & \rho_{1N}\\ \rho_{21} & \rho_{22} & \cdots & \rho_{2N}\\ \vdots & \vdots & & \vdots\\ \rho_{N1} & \rho_{N2} & \cdots & \rho_{NN}\end{bmatrix}. \tag{12}$$

During the identification interval T_d, node B detected N vehicles while node A found $N+\beta$ ($\beta\geq 0$) vehicles. The remaining β vehicles are postponed to the next identification interval T_{d+1}. For the elements in the correlation matrix $\boldsymbol{\Theta}$, the maximum $\rho_{i'j'}$ means vehicle j' and vehicle i' are the same vehicle. Set $\max(\rho_{i'j'})\geq\rho_{corr}$. If no qualifying $\rho_{i'j'}$ occurs, it means that there are errors in the identification process by nodes A and B, and error recognition is necessary. ρ_{corr} will be adjusted according to the actual requirements of experiments.

$E_8^A\rightarrow E_9^B$ is status 2 whose matching process is the same as in status 1.

E_{16}^A is status 3. After recognizing the remaining scenarios and errors, the next step is to discriminate the maximum value of the row vector in the correlation matrix $\boldsymbol{\Theta}$. If there is no row vector satisfying $\max(\rho_{i'j'})\geq\rho_{corr}$, then the vehicle represented by this row is recognized as merely entering without leaving.

E_3^A, $E_4^A\rightarrow E_3^B$, E_3^B are error (a), while E_5^A, $E_6^A\rightarrow E_6^B$, and $E_{11}^A\rightarrow E_{10}^B$, E_{11}^B are error (b). Error (a) is caused by the long body of a bus, which will make certain buses generate signals that overlap with datum line α. As a result, these buses are 'divided' into two passenger cars by a segmentation algorithm. Error (b) is caused by the close location between two consecutive passenger cars in congested traffic, which makes the segmentation algorithm fail to separate their signatures. To identify these two kinds of errors, after matching statuses 1 and 2, if the isolated signals that fail to be matched are adjacent on timeline, then the interval t_d can be judged as

$$t_d=t_{v,in}^n-t_{v-1,out}^n. \tag{13}$$

Calculating the intervals of the sample vehicle waveform, the shortest interval $t_{d,min}$ between two signature waveforms is 0.37 ms. That is to say, for all the waveforms obtained by one node, when t_d<0.3 ms, identification errors exist. To correct such errors, signatures need to be re-matched by combining E_v^N and E_{v+1}^N to $E_{v'}^N$.

After the above process, the vehicle signature matching between two nodes is completed, and each vehicle has a pair of signatures with a certain correlation.

3.4 Vehicle signature fusion

Through the fusion of a vehicle's signatures, a more accurate one can be obtained. After cross matching and error identification, each vehicle (except for the vehicles temporarily parked at a curb) has a pair of signatures. However, collecting and storing these signatures will generate errors and other uncertainties that affect the characterization of the vehicle signature. The fusion of vehicle signatures can reduce such negative effects. The fusion process uses a correlation function and maximum likelihood estimation.

The likelihood of each point of the vehicle signature is treated as an observation measurement, which is used to accomplish vehicle signature fusion. According to $\tilde{\delta}_n(t_{p,l}^n(k))=\tilde{\delta}(t_{p,l}^n(k)+\tau_n)+\omega_n$, vehicle signature E_v^N is treated as a stochastic process

$\{\tilde{\delta}_n(k)\}$ with a sample function of $\tilde{\delta}_n(k)$. Much statistics shows that the n-dimensional probability distribution of such a stochastic process is normally distributed. Its probability density function is shown as follows:

$$f_k(\tilde{\delta}_n(k))=\left(\frac{1}{\sqrt{2\pi}\sigma}\right)^{\|E_v\|+2\tau_n}\exp\left(-\frac{\left\|\tilde{\delta}_n-\tilde{\delta}_n(\tau_n)\right\|^2}{2\sigma^2}\right). \tag{14}$$

For nodes A and B, the observation of a same passenger car is defined as event $\boldsymbol{Z}$:

$$\boldsymbol{Z}=[\{\tilde{\delta}_A(k)\},\{\tilde{\delta}_B(k)\}]. \tag{15}$$

Therefore, for one vehicle, its signature distribution in the whole network is

$$f_k(Z(k))=\prod_{n=A,B} f_k(\tilde{\delta}_n(k)). \tag{16}$$

The logarithmic likelihood function of this distribution is

$$L(Z(k))=-(\|\boldsymbol{E}_v\|+2\tau_n)\ln(2\pi\sigma^2)-\sum_{n=A,B}\frac{\left\|\tilde{\delta}_n-\tilde{\delta}_n(\tau_n)\right\|^2}{2\sigma^2}. \tag{17}$$

The maximum likelihood estimation of vehicle signature $\tilde{E}_v^N$ is

$$\tilde{E}_v^N=\frac{1}{2}\sum_{n=A,B}\tilde{\delta}(t_{\mathrm{p},l}^n(k)+\tau_n). \tag{18}$$

The value of τ_n is determined as follows:

It can be concluded from previous discussion that $E_{i'}^A$ and $E_{j'}^B$ are the signatures for the same vehicle obtained by nodes A and B, respectively. The offset of these two signatures is defined as ω_{ij}, which can be estimated according to the cross-correlation of $E_{i'}^A$ and $E_{j'}^B$.

$$\omega_{ij}=\arg\max\left(\sum E_i^A E_j^B\right). \tag{19}$$

During waveform fusion, datum sampling is set as the signal obtained by either node A or node B, and the remaining signal's offset τ_n is ω_{ij}.

Therefore, for a vehicle detection network with two nodes A and B, the vehicle re-identification process can be described in the following steps:

Step 1: Map the sampling point time and the system time of each node.

Step 2: Use a dual-window vehicle detection algorithm to classify vehicles, and extract signatures of each vehicle.

Step 3: According to the correlation coefficient, cross match the vehicle signatures obtained by nodes A and B, and determine the vehicle status in the section.

Step 4: According to cross-correlation, determine the offset between two signature waveforms.

Step 5: Set the likelihood of a vehicle signature as the observation measurement, fuse the two signals via a maximum likelihood function, and obtain the ultimate vehicle signature.

Step 6: Use the ultimate vehicle signatures as the inputs of the vehicle identification algorithm and further identify vehicles.

4 Experiment results and analysis

The proposed multi-sensor spatio-temporal correlation algorithm is verified using video calibration data. There are two parts. The first part is to verify the signal processing by analyzing data obtained in one detection cycle. The accuracy of data collection and interpolation, the accuracy of cross matching, and the availability of waveform fusion results are the focus of this part. The second part is to verify the accuracy of vehicle re-identification. The verification is accomplished by comparing the results of inputting the original data and processed data, based on all the signatures obtained of the 19 369 vehicles.

4.1 Signal processing experiment

First, verify the accuracy of data storage and segmentation. A detection cycle T_d is 30 min. The verification data is collected from 7:00:00 to 7:05:00, Jan. 20, 2013. Fig. 4 shows the results of data collection.

According to the video calibration results, E_3^A is a bus, while E_{25}^A, E_{37}^A, and E_{54}^A are passenger cars. E_{54}^A is a special situation. Due to traffic congestion, the E_{54}^A vehicle has stopped for about 1.7 s when

passing node A. So, there is a section of the waveform approximately parallel with the datum line. Since this section will influence waveform matching, it is necessary to define it as a bad value. In the remaining processing, all bad values have to be found and removed after waveform segmentation. Algorithm 1 shows how to find and remove the bad values.

Fig. 5 shows the status comparison of E_{54}^{A}'s signature before and after being processed by Algorithm 1. It can be concluded from the comparison of the processed and unprocessed waveforms that, the bad value caused by the vehicle's stop is effectively removed by Algorithm 1. The comprehensive results of Figs. 4 and 5 justify that the algorithm of data storage and data segmentation is effective and can support the subsequent operations.

The next step is to verify the process of cross matching vehicle signatures obtained by nodes A and B.

Algorithm 1 Find and remove bad values

1 Determine the altitude difference $\Delta\tilde{\delta}$ between node n and node n+1

2 **If** $\Delta\tilde{\delta} < 20$
  Record these two points, n=n+1
  End if

3 **If** there has been a continuous appearance of more than 30 pairs of points which makes $\Delta\tilde{\delta} < 20$
  Remove the vehicle signatures of points that satisfy conditions from the first point n' to the last point n''
  End if

4 n=n''+1

5 Repeat step 2 until signal ends

In the 30 min detection cycle, among the signatures obtained by nodes A and B, the maximum waveform length $\|\boldsymbol{E}_v\|$ is 692. All the signatures obtained are normalized via the PCHIP algorithm through cross matching the waveform that has the maximum correlation coefficient. The results of cross matching are shown in Fig. 6.

Concluding from Fig. 6, within the detection cycle, there were 57 vehicles entering the section from node A, and 58 vehicles leaving from node B, 4 vehicles entering in the previous detection cycle, and

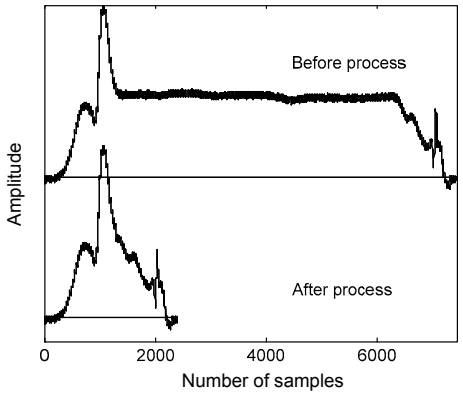

Fig. 5 The processing results of bad values caused by stop

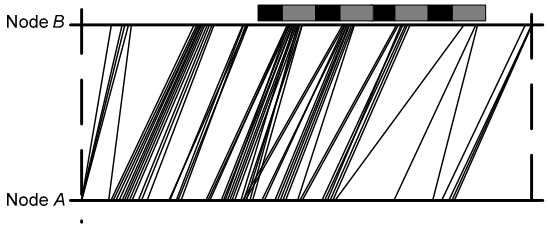

Fig. 6 The matching results of vehicles detected in one cycle

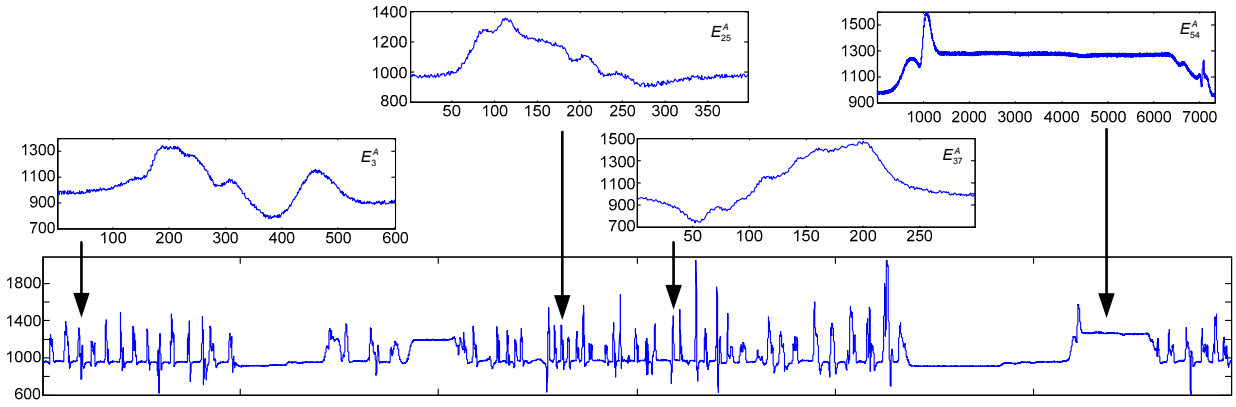

Fig. 4 The waveform obtained and its segmentation results of node A in a 30 min period (the x-axis represents the number of samples, and the y-axis represents amplitude)

3 vehicles not leaving at the end of this cycle. There were 13 vehicles that overtook the front vehicle before leaving. The 29th vehicle overtook the three consecutive vehicles ahead, and it had the largest amount of overtaking. Because of traffic congestion, node *A* misidentified the 14th and 15th passenger cars as a bus. After calibration, however, they were correctly matched with the corresponding vehicles at node *B*. During that detection cycle, there were two types of status, consistent with the previous discussion: (1) following the front vehicle until leaving the section; (2) overtaking one or more vehicles before leaving the section. To test the matching rate, data obtained during the time period 6:00:00 to 10:00:00, Jan. 20, 2013 was chosen to check the accuracy. All the matching results were calibrated with video recognition data. During the 8 detection cycles, there were a total of 902 vehicles which entered the experimental section, 896 vehicles left, 3 stopped at the temporary parking curb, and 1 left from the temporary parking curb. The matching rate was 98.97%, which is much higher than those of the existing identification algorithms. Therefore, the matching result is qualified for the remaining processing by comparing the proposed algorithm with other typical algorithms for vehicle re-identification (Table 2). The higher accuracy is mainly due to the fact that our algorithm considers the vehicle status on the road and corrects errors cause by a single node.

Table 2 The matching rate of several algorithms

Algorithm	Matching rate (%)
VSMA	95.60
CM	93.80
DTW	78.00
AG4	92.00
STC	**98.97**

VSMA is an algorithm proposed for the Intelligent Imaging Systems (Ndoye *et al*., 2011a), CM was designed by Sensys Networks, Inc. (Kwong *et al*., 2010), DTW was developed by a team from the University of Arizona (Lin and Tong, 2011), AG4 was proposed by a research team from UC Berkeley (Sanchez *et al*., 2011), and STC stands for the algorithm proposed in this paper

With increase in the sample volume, Fig. 6 shows more details of the traffic flow than Fig. 3. The most significant feature is that Fig. 6 shows the split of node *B*, which is also consistent with the matching result of Kwong *et al*. (2009). Therefore, the matching process is successful and appropriate.

About the result of the fusion process, a vehicle's signatures have been taken as an example. Fig. 7 shows the signatures of a vehicle obtained by nodes *A* and *B*, as well as the fusion result. The lengths of the waveforms obtained by nodes *A* and *B* are equal because all signatures have been normalized during the matching process. However, the offset caused by the different speeds of the vehicles and environmental noise still exists. The first peak of the signature waveform obtained by node *B* comes earlier than that obtained by node *A*. After interpolation, the last peaks of both waveforms are essentially coincident. Meanwhile, the waveform of node *B*'s signature has more glitches, mainly because node *B* suffers from stronger interference by using maximum likelihood estimation to fuse the signature data, setting the waveform of node *A* as the datum, and obtaining the ultimate signature waveform. It can be concluded that, the fusion result keeps some details of the signatures well, and the curve is smoother than those of the original signals since the interference is filtered by the fusion algorithm.

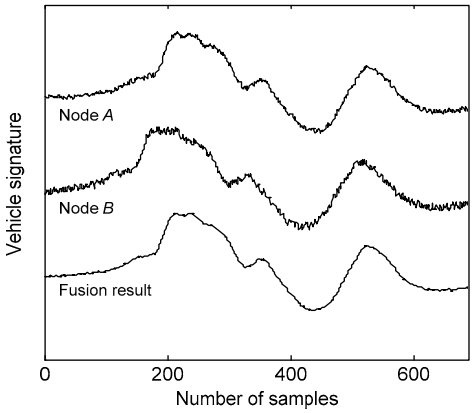

Fig. 7 Two signature waveforms of a same vehicle and the fusion result

Concerning the error (a) discussed in Section 3.3, Fig. 8 shows the signatures and fusion results of two vehicles passing nodes *A* and *B*.

Video calibration shows that, when these two passenger cars passing node *B* are near each other, the identification algorithm misidentifies them as a bus. When passing node *A*, they are far from each other and have separate signature waveforms. The proposed algorithm can solve this problem by fusing vehicle signatures according to the spatio-temporal correlations of signals from nodes *A* and *B*.

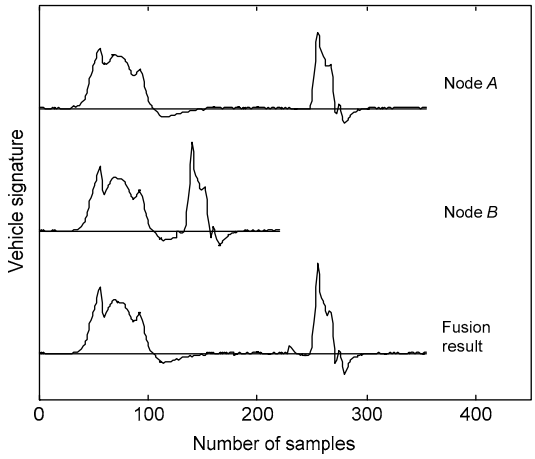

Fig. 8 A kind of recognition error caused by a single node and the result of multi-sensor node fusion

4.2 Effectiveness of the algorithm

The effectiveness of the proposed algorithm is verified by comparing the results of single node identification and multi-node re-identification, setting all data from the experimental sample as the input parameters (Table 3). The standard of vehicle identification is referred to the FHWA (Federal Highway Administration, USA) scheme.

Table 3 Comparison between the identification results of single node identification and multi-node re-identification

Vehicle type	Actual number of vehicles	Number of vehicles correctly identified		Accuracy	
		Single node	Multi-node	Single node	Multi-node
Bus	1284	996	1192	77.6%	92.8%
Car	15668	15088	15213	96.3%	97.1%
Truck	516	384	420	74.4%	81.4%
Van	1888	1736	1781	91.9%	94.3%
Total	19356	18204	18606	94.0%	96.1%

Table 3 shows that, with the joining of the second detection node, the accuracy of vehicle identification has been significantly improved. Such progress is especially significant in bus identification. Although the accuracy has been improved, errors caused mainly by matching failures still exist. The reason for these failures can be analyzed from video calibration, and is generalized as follows: When overtaking, a vehicle needs to leave its current lane, and goes back to the original lane after overtaking. Such a lane change is common in daily driving. If it happens just at node *A* or *B*, however, the headway direction of the vehicle will have a large offset from the *x*-axis (Fig. 9). A large difference will occur between the actual waveform and the waveform obtained, and vehicle matching fails.

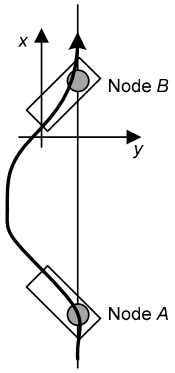

Fig. 9 The driving line of a vehicle which leads to a matching failure

The situation described in Fig. 9 is an extreme phenomenon: a vehicle leaves the lane obliquely when it is passing node *A*, and enters the lane obliquely when passing node *B*. Such a scenario is unlikely to actually happen. Only entering or only leaving obliquely, however, is possible. It is shown by statistics that among the 19368 vehicles detected, 419 vehicles (2.16% of the whole sample) had obliquely entered or left when passing node *A* or *B*. There are two methods to address such matching errors. One is to add two sensors at each side of each existing node. The three nodes cooperate horizontally and make sure that certain vehicles have left the lane. The other is to determine the vehicle status by analyzing the outputs of the *x*-axis and *y*-axis. The latter is the direction of our future research.

5 Conclusions

In this paper we propose a method to re-identify vehicles by using the correlation of signatures from multiple sensor nodes. This method can provide more effective inputs for existing vehicle identification algorithms, and thus improves the accuracy of vehicle identification. It uses multiple sensor nodes to identify one vehicle for several times, which reduces errors caused by interference such as vehicle distance, speed, and environmental noise.

The proposed algorithm uses a wireless sensor network consisting of magnetic sensor nodes, so it is

cost saving and easy to lay out. Also, the information obtained is limited to vehicle signatures, so there is little privacy offence.

The proposed algorithm can obtain vehicle status information with higher accuracy. Experiments show that by cross matching vehicle signatures, this method can effectively distinguish vehicle statuses such as following, overtaking, and temporal stopping, by using the cross-correlation of signatures to correct the offset. Furthermore, the signatures obtained are fused by applying maximum likelihood estimation, which reduces the random error in a single-point sensor system.

Based on the data of the 19368 practically measured vehicles, the vehicle re-identification algorithm can effectively improve the accuracy of vehicle identification, especially for buses. The matching rate is 98.97%. The accuracy of vehicle identification is 96.1%, which is 2.1% higher than that of the algorithms using a single node under the same conditions. The accuracy of bus identification increases by 15.2%.

Although the proposed approach can effectively improve the accuracy of vehicle identification, it is still immature for practical applications. The focus of research in the next stage is to make the vehicle re-identification algorithm adapt to actual traffic flow with highly complex and random composition.

References

Abdulhai, B., Tabib, S.M., 2003. Spatio-temporal inductance-pattern recognition for vehicle re-identification. *Transp. Res. Part C Emerg. Technol.*, **11**(3):223-239. [doi:10.1016/S0968-090X(03)00024-X]

Ahmed, M.M., Abdel-Aty, M.A., 2012. The viability of using automatic vehicle identification data for real-time crash prediction. *IEEE Trans. Intell. Transp. Syst.*, **13**(2):459-468. [doi:10.1109/TITS.2011.2171052]

Cheung, S.Y., Varaiya, P.P., 2007. Traffic Surveillance by Wireless Sensor Networks: Final Report. California PATH Program, Institute of Transportation Studies, University of California at Berkeley.

Cheung, S.Y., Coleri, S., Dundar, B., *et al.*, 2005. Traffic measurement and vehicle classification with single magnetic sensor. *J. Transp. Res. Board*, **1917**(1):173-181. [doi:10.3141/1917-19]

Coifman, B., 1998. Vehicle re-identification and travel time measurement in real-time on freeways using existing loop detector infrastructure. *J. Transp. Res. Board*, **1643**(1):181-191. [doi:10.3141/1643-22]

Fritsch, F.N., Carlson, R.E., 1980. Monotone piecewise cubic interpolation. *SIAM J. Numer. Anal.*, **17**(2):238-246. [doi:10.1137/0717021]

Gandhi, T., Trivedi, M.M., 2006. Panoramic appearance map (PAM) for multi-camera based person re-identification. IEEE Int. Conf. on Video and Signal Based Surveillance, p.78. [doi:10.1109/AVSS.2006.90]

Gunay, B., 2012. Using automatic number plate recognition technology to observe drivers' headway preferences. *J. Adv. Transp.*, **46**(4):305-317. [doi:10.1002/atr.1197]

Haoui, A., Kavaler, R., Varaiya, P., 2008. Wireless magnetic sensors for traffic surveillance. *Transp. Res. Part C Emerg. Technol.*, **16**(3):294-306. [doi:10.1016/j.trc.2007.10.004]

Kaewkamnerd, S., Pongthornseri, R., Chinrungrueng, J., *et al.*, 2009. Automatic vehicle classification using wireless magnetic sensor. IEEE Int. Workshop on Intelligent Data Acquisition and Advanced Computing Systems: Technology and Applications, p.420-424. [doi:10.1109/IDAACS.2009.5342949]

Keawkamnerd, S., Chinrungrueng, J., Jaruchart, C., 2008. Vehicle classification with low computation magnetic sensor. 8th Int. Conf. on ITS Telecommunications, p.164-169. [doi:10.1109/ITST.2008.4740249]

Kwong, K., Kavaler, R., Rajagopal, R., *et al.*, 2009. Arterial travel time estimation based on vehicle re-identification using wireless magnetic sensors. *Transp. Res. Part C Emerg. Technol.*, **17**(6):586-606. [doi:10.1016/j.trc.2009.04.003]

Kwong, K., Kavaler, R., Rajagopal, R., *et al*., 2010. Real-time measurement of link vehicle count and travel time in a road network. *IEEE Trans. Intell. Transp. Syst.*, **11**(4):814-825. [doi:10.1109/TITS. 2010.2050881]

Lin, W.H., Tong, D., 2011. Vehicle re-identification with dynamic time windows for vehicle passage time estimation. *IEEE Trans. Intell. Transp. Syst*., **12**(4):1057-1063. [doi:10.1109/TITS. 2011.2140318]

Lotufo, R.A., Morgan, A.D., Johnson, A.S., 1990. Automatic number-plate recognition. IEE Colloquium on Image Analysis for Transport Applications, p.6/1-6/6.

Ndoye, M., Totten, V.F., Krogmeier, J.V., *et al.*, 2011a. Sensing and signal processing for vehicle reidentification and travel time estimation. *IEEE Trans. Intell. Transp. Syst.*, **12**(1):119-131. [doi:10.1109/TITS.2010.2092769]

Ndoye, M., Barker, A.M., Krogmeier, J.V., *et al.*, 2011b. A recursive multiscale correlation-averaging algorithm for an automated distributed road-condition-monitoring system. *IEEE Trans. Intell. Transp. Syst.*, **12**(3):795-808. [doi:10.1109/TITS.2011.2132799]

Sanchez, R.O., Flores, C., Horowitz, R., *et al.*, 2011. Vehicle re-identification using wireless magnetic sensors: algorithm revision, modifications and performance analysis. IEEE Int. Conf. on Vehicular Electronics and Safety, p.226-231. [doi:10.1109/ICVES.2011.5983819]

Sharma, A., Bullock, D.M., Bonneson, J.A., 2007. Input-output and hybrid techniques for real-time prediction of delay and maximum queue length at signalized intersections. *J. Transp. Res. Board*, **2035**(1):69-80. [doi:10.3141/2035-08]

Tam, M.L., Lam, W.H., 2011. Application of automatic vehicle identification technology for real-time journey time estimation. *Inform. Fusion*, **12**(1):11-19. [doi:10.1016/j.inffus.2010.01.002]

Zhang, W., Tan, G., Ding, N., *et al.*, 2008. Vehicle classification algorithm based on binary proximity magnetic sensors and neural network. 11th Int. IEEE Conf. on Intelligent Transportation Systems, p.145-150. [doi:10.1109/ITSC.2008.4732522]